Near-band-gap reflectance anisotropy in ordered $Ga_{0.5}In_{0.5}P$

J. S. Luo, J. M. Olson, Yong Zhang, and A. Mascarenhas
National Renewable Energy Laboratory, Golden, Colorado 80401
(Received 19 September 1996)

We present a theory that models the reflectance difference spectrum of bulk, spontaneously ordered $Ga_{0.5}In_{0.5}P$. Near the band gap E_0 this spectrum exhibits a sharp, negative feature at E_0 and a broad positive feature that peaks near $E_0+\Delta_S$. The zero crossing between these two peaks occurs near $E_0+\Delta_C$. For the sample studied in this paper, the spin-orbit splitting Δ_s and the crystal-field splitting Δ_C are 120 and 25 meV, respectively. Two previous calculations, which assume constant transition-matrix elements, were able to produce a negative peak at E_0, but not the positive feature. In this paper, the reflectance difference spectrum near the band gap is calculated using an 8-band $\mathbf{k}\cdot\mathbf{p}$ model and an explicit treatment of the momentum or $\mathbf{k}$ dependence of the transition-matrix elements. The new calculation produces both the negative peak at E_0 and the positive feature that peaks near $E_0+\Delta_S$. The positive feature is attributed to the strong $\mathbf{k}$ dependence of the matrix element anisotropy. A strong coupling, enhanced by ordering, between three valence bands is essential. A problem associated with the analytical expression for the dielectric function ε used in previous calculations is discussed. [S0163-1829(97)07224-X]

I. INTRODUCTION

Spontaneous ordering in III-V materials has been studied extensively in recent years. For $Ga_{0.5}In_{0.5}P$ the most frequently observed form of ordering consists of alternating planes of $Ga_{0.5+\eta/2}In_{0.5-\eta/2}P$ and $Ga_{0.5-\eta/2}In_{0.5+\eta/2}P$ in the [111] direction where η is the order parameter. This form of ordering is often referred to as CuPt-like. Associated with the ordering are two major electronic features: (1) the band gap E_0 is reduced,[1] in some cases by more than 100 meV (Refs. 2 and 3) at the Γ point, the valence-band maximum, fourfold degenerate in disordered $Ga_{0.5}In_{0.5}P$, is split[4] with an energy difference Δ_C. Theoretically, the ordering-induced shift of the band gap,[5] ΔE_0, and the valence-band splitting,[6] Δ_C, are to first order, quadratic functions of η. This implies that for samples with weak ordering ($\eta \ll 1$), detection of ordering in $Ga_{0.5}In_{0.5}P$ by traditional optical techniques is difficult. This is consistent with previous experimental work using photoluminescence (PL),[4,7,8] photoluminescence excitation (PLE),[7–10] and modulated reflectance[11–14] to measure ΔE_0 and Δ_C. Recently, however, reflectance difference spectroscopy (RDS) has been shown to be a more sensitive technique for detecting the presence of ordering in III-V alloys and can easily be adapted to *in situ* measurements during and after growth.[15–17]

II. BACKGROUND

RDS measures the anisotropy of optical reflectance. In this study we let

$$\Delta R/R = \frac{(R_{1\bar{1}0}-R_{110})}{(R_{1\bar{1}0}+R_{110})/2}, \tag{1}$$

where $R_{1\bar{1}0}$ and R_{110} are the reflectances along $[\bar{1}10]$ and [110], respectively. Originally, RDS was used to study the anisotropic surface reconstruction of III-V materials with isotropic bulk properties.[18] The RD spectrum of an ordered III-V alloy generally exhibits both surface- and bulk-induced spectral features and, at times, it is difficult to separate the two effects.[15,16] Recently, however, we have developed a technique for effectively quenching the surface-induced features in ordered $Ga_{0.5}In_{0.5}P$.[19] (In short, this is accomplished by annealing the $Ga_{0.5}In_{0.5}P$ in H_2 at a temperature of about 400 °C to achieve a group-III terminated surface and then exposing this surface to N_2 or air at room temperature.)

A typical *bulk* RD spectrum of (partially) ordered $Ga_{0.5}In_{0.5}P$ is shown in Fig. 1. The important ordering-related RDS features are (1) a sharp, negative feature at E_0, (2) a broad, positive feature that peaks at $E_0+\Delta_S$, and (3) a zero crossing between the two peaks that occurs near $E_0+\Delta_C$. The sample of Fig. 1 was grown by metalorganic chemical vapor deposition using PH_3, trimethylgallium, and trimethylindium in a H_2 carrier gas. The input P to (In+Ga) ratio during growth was 60, and the growth temperature and rate were 670 °C and 5.5 μm/h, respectively. The layer was grown on a (001) GaAs substrate misoriented 6° toward (111)B. Details of the growth setup are described elsewhere.[15] The sample was specularly smooth and closely lattice matched ($\Delta a/a < 10^{-3}$) to the underlying GaAs substrate. It contained a single CuPt-like ordering variant and the background doping density was below 10^{16} cm^{-2}, *n*-type. These properties avoid complications introduced by strain effects,[20] electro-optic effects[21] associated with heavy doping, and anisotropic surface roughness effects associated with two-variant ordered $Ga_{0.5}In_{0.5}P$.[15,22,23]

The observed optical anisotropy near E_0 has been investigated theoretically using 4-band[15,16] and 6-band[24] Luttinger models, where ordering related terms were added to the Hamiltonian by treating the effect of ordering in the same way that one would treat the effect of uniaxial strain. Both strain and/or ordering reduce the crystal symmetry and split the valence-band maximum. The 4- and 6-band models yield expressions for $\Delta R/R$ in terms of the band energies E_i (i.e., E_0, $E_0+\Delta_C$, and $E_0+\Delta_S$) that characterize the effects of ordering in the material. These expressions are of the form

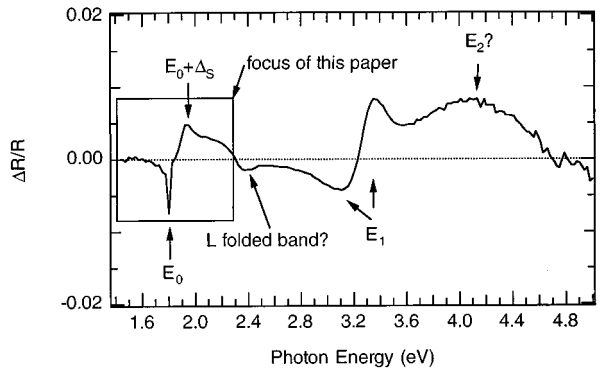

FIG. 1. Experimental RD spectrum of ordered $Ga_{0.5}In_{0.5}P$. The theory developed in this paper is only valid for photon energies in the vicinity of E_0 and $E_0+\Delta_S$.

$$\frac{\Delta R}{R}=-\frac{c_0}{E^2}\sum_i a_i\sqrt{E_i-E}, \tag{2}$$

where c_0 is a constant and $a_i=M^2_{i,(1\bar{1}0)}-M^2_{i,(110)}$ is the momentum matrix element anisotropy for the ith transition at energy E_i. (In this paper, we use the convention that the $\sqrt{x}=0$ if $x<0$.) For the 6-band model $a_0=-(a_1+a_2)$ and a_1 and a_2 are functions of η. For the 4-band model, it was assumed that $\eta\ll 1$, and, as a consequence, $a_2\cong 0$ and $a_0\cong -a_1$. The line shapes predicted by Eq. (2) (solid line) for the 4- and 6-band models are plotted in Figs. 2(a) and 2(b), respectively. The 4-band model[15,16] neglects the ordering-induced coupling between the crystal-field and the spin-orbit slit-off bands while the 6-band model[24] includes this coupling in the calculation of the matrix elements and energy levels. Although both models produce a negative peak at E_0, neither is a good fit to the experimental line shape and neither reproduces the positive feature at $E_0+\Delta_S$. One problem with both models is that the functional form of Eq. (2) (related to the form of ε_1) is only accurate for photon energies near the critical point and for weakly ordered alloys. The more accurate function form (see the Appendix) is

$$\frac{\Delta R}{R}=-\frac{c_0}{E^2}\sum_i a_i(2\sqrt{E_i}-\sqrt{E_i+E}-\sqrt{E_i-E}) \tag{3}$$

shown as thin lines in Figs. 2(a) and 2(b). The fits, using Eq. (3), are somewhat better for photon energies less than E_0 but are still lacking for energies greater than E_0. We show in the following that the problem with both models [and with Eq. (3)] is the assumption that the matrix element anisotropy $a_i=M^2_{i,(1\bar{1}0)}-M^2_{i,(110)}$ is independent of $\mathbf{k}$.

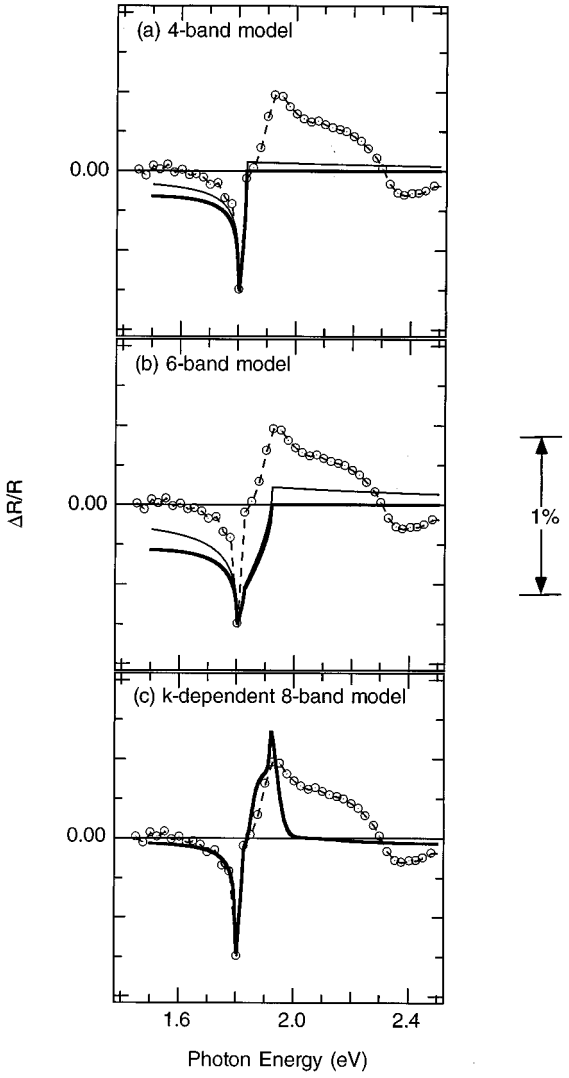

FIG. 2. RD spectrum (open circle) and model calculations (thick lines): (a) 4-band model (Ref. 15), (b) 6-band model (Ref. 24), and (c) 8-band $\mathbf{k}\cdot\mathbf{p}$ model (this study). By varying c_0, the intensities of the RDS line shapes in (a), (b), and (c) are adjusted to fit the experimental intensity at E_0. The dashed line going through the data points is a guide to the eye. Although the resolution at E_0 is ± 25 meV, spectra measured with higher resolution produce essentially the same line shape as that represented by the dashed line. The thin solid lines in (a) and (b) are line shapes calculated using the correct ε line shape for the 4- and 6-band models.

III. THEORY

In this paper, a new RDS calculation using an eight-band $\mathbf{k}\cdot\mathbf{p}$ model is presented. The $\mathbf{k}$ dependence of the transition matrix elements is treated explicitly. This idea was stimulated by the work of O'Reilly and Meney.[25] They calculated the valence subband dispersion in strained quantum wells of ordered $Ga_{0.5}In_{0.5}P$ and showed that the optical transition matrix elements are strongly anisotropic over a large region of $\mathbf{k}$ space. They also found that ordering plays a significant role in the coupling between the three valence subbands. More recently, Zhang and Mascarenhas[26] have shown that the $\mathbf{k}$ dependence of the matrix elements significantly affects the polarization of the excitonic states in ordered III-V alloys. Consequently, the usual assumption that the transition matrix element anisotropy is independent of $\mathbf{k}$ is suspect. A treatment of the RDS problem using the $\mathbf{k}$ dependence of matrix element anisotropy and the correct functional form for ε_1 is discussed below. We show that this model is a much better fit to the RD spectrum of ordered $Ga_{0.5}In_{0.5}P$ around E_0. More importantly, we show that the effect of the

order-induced coupling between the *three* valence bands at $\mathbf{k}\neq 0$ cannot be neglected.

From the standard Fresnel equation for normal incidence reflectance, $R=|(\sqrt{\varepsilon}-1)/(\sqrt{\varepsilon}+1)|^2$, we first express Eq. (1) in a more general form,

$$\Delta R/R=f(\varepsilon_1,\varepsilon_2)\Delta\varepsilon_1+g(\varepsilon_1,\varepsilon_2)\Delta\varepsilon_2, \tag{4}$$

where the dielectric function $\varepsilon=(\varepsilon^{1\bar{1}0}+\varepsilon^{110})/2=\varepsilon_1+i\varepsilon_2$, and $\Delta\varepsilon_j=(\varepsilon_j^{1\bar{1}0}-\varepsilon_j^{110})$, $j=1$ or 2. [Only linear terms in $\Delta\varepsilon_1$ and $\Delta\varepsilon_2$ are retained in the differentiation leading to Eq. (4).] In order to include the $\mathbf{k}$ dependence of the matrix elements, we use the following integral expressions for $\Delta\varepsilon_1$ and $\Delta\varepsilon_2$:[27,28]

$$\Delta\varepsilon_1=\sum_i(\Delta\varepsilon_1)_i=\sum_i\frac{2}{\pi}\frac{c_0}{(E_i)^{(3/2)}}\int_0^{x_m}\frac{a_i(x)\sqrt{x}}{[(1+x)^2-\zeta_i^2](1+x)}\,dx, \tag{5a}$$

$$\Delta\varepsilon_2=\sum_i(\Delta\varepsilon_2)_i=\sum_i\frac{c_0}{(E_i)^{(3/2)}}\int_0^{x_m}\frac{a_i(x)\sqrt{x}[\delta(1+x-\zeta_i)+\delta(1+x+\zeta_i)]}{(1+x)^2}\,dx$$

$$=\sum_i\frac{c_0}{(E_i)^{(3/2)}\zeta_i^2}[a_i(\zeta_i-1)\sqrt{\zeta_i-1}-a_i(-\zeta_i-1)\sqrt{-\zeta_i-1}], \tag{5b}$$

where the anisotropic parameters $a_i(x)=M^2_{i,(1\bar{1}0)}-M^2_{i,(110)}$ have the same meaning as described above, $\zeta_i=(\hbar\omega/E_i)$, and $x_m=\hbar^2\mathbf{k}_m^2/2\mu E_i$. Here, we ignore the detailed shape of the Brillouin zone by replacing it with a sphere of radius $\mathbf{k}_m$. We let x_m be an arbitrarily large number and we set $a_i(x>0.4)=a_i(x=0.4)$.

The $\mathbf{k}$ dependence of $a_i=\Delta M_i^2$ is calculated using an eight-band $\mathbf{k}\cdot\mathbf{p}$ model.[26,20] For each transition, the result is calculated for $\mathbf{k}$ up to 1/5 Brillouin zone and averaged over $\mathbf{k}$ parallel and perpendicular to the ordering direction. The density of states reduced masses for the three valence subbands have been found to be very similar[26] and are assumed to be equal to $\mu=(\mu_\perp^2\mu_\parallel)^{1/3}$ for all three transitions. The result, as a function of $x=\hbar^2\mathbf{k}^2/2\mu E_i$, is shown in Fig. 3. It is clearly seen in Fig. 3 that the transition matrix elements anisotropies a_0, a_1, and a_2 for the three subbands are strong functions of $\mathbf{k}$. The coupling is mostly ordering induced because the top of the valence band, in the spherical approximation, does not couple with two other valence bands in the zinc-blende structure when $\mathbf{k}\neq 0$.[29]

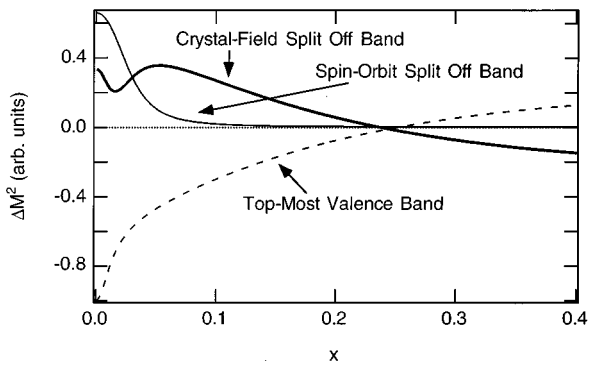

FIG. 3. ΔM^2 vs $x=(\hbar^2\mathbf{k}^2/2\mu E_i)$ for transitions between the valence bands and the conduction band. Because of ordering, the three valence-band states are mixtures of the original unperturbed heavy-hole, light-hole, and spin-orbit states. The labels used here should not be taken literally and are used for reference only.

Although the $\mathbf{k}\cdot\mathbf{p}$ method for calculating $E_i(\mathbf{k})$ and M_i^2 becomes less accurate for large values of $\mathbf{k}$, it is nevertheless reasonably accurate for calculating ΔM_i^2. This is illustrated in Fig. 3, where, for photon energies far from the band edge, ΔM_i^2 approaches zero, as expected, since the ordering mainly perturbs the band structure in an energy range comparable to the crystal-field splitting. Similarly, this model should be more accurate for calculating $\Delta\varepsilon_i$ than ε_i. It is worth mentioning that this approach reduces to the expected limits: at $\mathbf{k}=0$, the a_i's are equal to those calculated in the 6-band model, and if we let $a_i(x)=a_i(x=0)$, Eq. (3) is obtained from Eqs. (4) and (5a). Also, if we replace ΔM_i^2 with M_i^2 in Eqs. (5a) and (5b), we then obtain the correct one-electron expressions for ε_1 and ε_2, respectively.

IV. DISCUSSION

Several other important assumptions are made in this new calculation. (1) In principle, ε is a tensor for uniaxial $Ga_{0.5}In_{0.5}P$. Here, the ordering effect has been treated as a perturbation of ε_i. (2) We assume the functional forms of ε_1 and ε_2 are not sensitive to the ordering-induced coupling between the valence bands. This has been observed by Phillips *et al.*[17] and this assumption is also made in the 4- and 6-band models. (3) Equations (5a) and (5b) are in the framework of the parabolic approximation and ignore any nonparabolicity[26] in the valence bands at $\mathbf{k}\neq 0$. (4) We have ignored the contributions of the higher conduction and valence bands, which may contribute to the RD intensity for $E>E_0+\Delta_S$. (5) We have also ignored the influence of excitonic effects on the ε line shape.[30]

The line shape predicted by this work (solid line) is plotted along with the experimental spectrum in Fig. 2(c). Compared to the line shapes from the 4- and 6-band models [Figs. 2(a) and 2(b)], the line shape calculated in this paper not only fits better the data below E_0, but also reproduces a portion of the positive feature at $E_0+\Delta_S$. Figure 3 shows the negative peak at E_0 is mainly due to the anisotropy of the topmost or heavy-hole-like valence band. The contributions

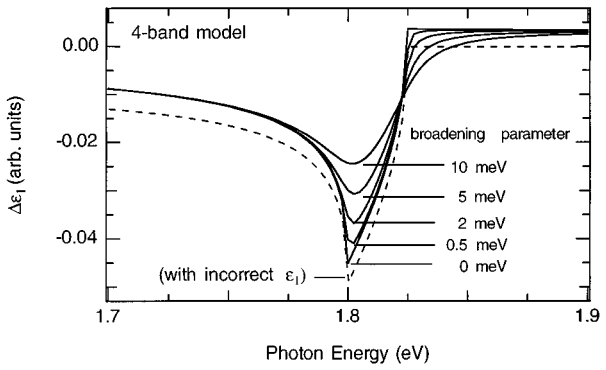

FIG. 4. Results of $\Delta\varepsilon_1$ vs energy using the functional form of Kato *et al.* (Ref. 32) for a series of different line broadening parameters, Γ_0.

from the other two bands are positive at E_0. The positive RDS feature at $E_0+\Delta_S$ is due mainly to the spin-orbit split-off band modulated by strong, ordering-induced coupling between the valence bands for $\mathbf{k}\neq 0$. This also suggests that the cause of the poorer fit in the 6-band model relative to this model is due to (1) neglecting the off zone center ($\mathbf{k}\neq 0$) coupling and (2) the use of an incorrect expression for the ε_1 line shape. It is worth mentioning that the contribution to the RDS intensity for all three models from ε_2 is negligible for $E<E_0+\Delta_S$.

In a previous work, Luo *et al.*[16,31] showed experimentally that the RD peak intensity at E_0, $\Delta R/R|_{E_0}$, varied linearly with $\sqrt{\Delta E_0}$ where $\Delta E_0(\propto\eta^2)$ is the ordering-induced band-gap shift. The 4-band model (in the limit of $\eta\ll 1$) yields this result explicitly. The 6-band model yields a superlinear relationship between $\Delta R/R|_{E_0}$ and $\sqrt{\Delta E_0}$ (or η) due to ''intensity borrowing'' between the three valence subbands. In this work, we have not calculated the η dependence of $\Delta R/R|_{E_0}$ but simply wish to point out that both the 4-band and 6-band models are not likely to produce the correct functional dependence for *finite* η because of the incorrect ε line shape and the $\mathbf{k}$ dependence of ΔM_i^2. If the correct line shape is used, the 6-band model, for a given η, overestimates the RDS intensity at E_0 compared to the current 8-band model. Furthermore, at least theoretically, the peak intensity is also affected by line broadening effects. This is shown in Fig. 4. Here, we simulate line broadening effects by using a more general and accurate expression for the dielectric function,[32] which explicitly includes a line broadening parameter Γ_0:

$$(\varepsilon)_i=\varepsilon_0+M_i^2 c_0 E_i^{-1.5}\chi_i^{-2}(2-\sqrt{1+\chi_i}-\sqrt{1-\chi_i}), \quad (6)$$

where $\chi_i=(E+i\Gamma_0)/E_i$. Since the $\Delta R/R$ line shape is dominated by the $\Delta\varepsilon_1$ term we only plot $\Delta\varepsilon_1$. Using a modified form of the 4-band model (with $a_0=-a_{CF}$), Fig. 4 shows that the intensity of $\Delta\varepsilon_1$ decreases by a factor of 2 by varying the broadening parameter from 0 to 10 meV. A value of 59 meV was used by Kato *et al.*[32] for fitting ellipsometry data of $Ga_{0.5}In_{0.5}P$. (The importance of line broadening in the study of the optical properties of semiconductors has also been pointed out by Tanguy.[30]) This may be the cause for the relatively large amount of scatter in the data used to construct the plot of $\Delta R/R|_{E_0}$ versus $\sqrt{\Delta E_0}$ by Luo *et al.*[16,31] (We conjecture that the wide range of growth conditions required to yield a variety of samples with widely different band gaps also leads to samples with widely different broadening parameters.) Finally we would like to point out that although the theory presented in this paper does at least qualitatively reproduce both the negative peak at E_0 and the positive peak at $E_0+\Delta_S$, there is still a shoulder on the high-energy side of the latter that remains unexplained. It may be related to the folded L band. Work is continuing in an effort to explain quantitatively the origin of this spectral feature.

V. CONCLUSION

In conclusion, we have presented a model using an 8-band $\mathbf{k}\cdot\mathbf{p}$ theory that yields an RDS line shape near E_0 comparable to that which is observed experimentally. The success of this models depends critically on the explicit treatment of the $\mathbf{k}$ dependence of the transition-matrix elements. In particular, the *strength and the line shape* of the spin orbit feature are primarily determined by the ordering-induced $\mathbf{k}$-dependent anisotropy of the transition-matrix element. We have also pointed out that, to test an RDS model, a line-shape comparison to the experimental data is more meaningful than a single point measurement or calculation of intensity at some critical point. A discussion related to the incorrect functional form of ε_1 used in previous calculations is given in the Appendix.

ACKNOWLEDGMENTS

We would like to thank Sarah Kurtz, S.-H. Wei, and W. McMahon for helpful discussions. This work is supported by the Office of Energy Research, Basic Energy Sciences, Department of Energy.

APPENDIX

As noted earlier, the functional form of ε_1 (and $\Delta\varepsilon_1$) used in both the 4- and 6-band models is incorrect due to an incorrect Kramers-Kronig transformation. The fundamental physical requirements for both ε_1 and ε_2 are[28,30]

$$\varepsilon_1(E)=\varepsilon_1(-E) \quad \text{(even function)}, \quad (A1)$$

$$\varepsilon_2(E)=-\varepsilon_2(-E) \quad \text{(odd function)}. \quad (A2)$$

The correct functional forms of $\Delta\varepsilon_1$ and $\Delta\varepsilon_2$ that satisfy Eqs. (A1) and (A2), and Kramers-Kronig (KK) relations can be obtained from Eqs. (5a) and (5b) by ignoring the $\mathbf{k}$ dependence of a_i:[27,28]

$$[\Delta\varepsilon_2(E)]_i=\begin{cases}(a_i c_0/E^2)\sqrt{E-E_1}, & E\geqslant E_i,\\ 0, & -E_i<E<E_i,\\ -(a_i c_0/E^2)\sqrt{-E-E_i}, & E<-E_i,\end{cases} \quad (A3)$$

$$[\Delta\varepsilon_1(E)]=\varepsilon_0+(a_i c_0/E^2)(2\sqrt{E_i}-\sqrt{E_i+E}-\sqrt{E_i-E}). \quad \text{(A4)}$$

Only the $E>0$ part of Eq. (A4) was used by the 4- and 6-band models. Although this omission violates the condition of Eq. (A2), it has no effect on the physical correctness of $\Delta\varepsilon_2$. However, it has a significant effect on the KK transformation of $\Delta\varepsilon_2$ to $\Delta\varepsilon_1$. Consequently, Eq. (2) (which is proportional to $\Delta\varepsilon_1$) violates the requirement described in Eq. (A1).

[1] A. Gomyo, T. Suzuki, K. Kobayashi, S. Kawata, I. Hino, and T. Yuasa, Appl. Phys. Lett. **50**, 673 (1987).

[2] M. C. DeLong, P. C. Taylor, and J. M. Olson, Appl. Phys. Lett. **57**, 620 (1990).

[3] M. K. Lee, R. H. Horng, and L. C. Haung, J. Cryst. Growth **124**, 358 (1992).

[4] A. Mascarenhas, S. Kurtz, A. Kibbler, and J. M. Olson, Phys. Rev. Lett. **63**, 2108 (1989).

[5] R. B. Capaz and B. Koiller, Phys. Rev. B **47**, 4044 (1993).

[6] D. B. Laks, S. H. Wei, and A. Zunger, Phys. Rev. Lett. **69**, 3766 (1992).

[7] D. J. Mowbray, R. A. Hogg, M. S. Skolnick, M. C. DeLong, S. R. Kurtz, and J. M. Olson, Phys. Rev. B **46**, 7232 (1992).

[8] M. C. DeLong, D. J. Mowbray, R. A. Hoggs, M. S. Skolnick, M. Hopkinson, J. P. R. David, P. C. Taylor, S. R. Kurtz, and J. M. Olson, J. Appl. Phys. **73**, 5163 (1993).

[9] G. S. Horner, A. Mascarenhas, S. Froyen, R. G. Alonso, K. Bertness, and J. M. Olson, Phys. Rev. B **47**, 4041 (1993).

[10] P. Ernst, C. Geng, F. Scholz, H. Schweizer, Y. Zhang, and A. Mascarenhas, Appl. Phys. Lett. **67**, 2347 (1995).

[11] S. R. Kurtz, J. M. Olson, and A. Kibbler, Solar Cells **24**, 307 (1988).

[12] S. R. Kurtz, J. Appl. Phys. **74**, 4130 (1993).

[13] R. G. Alonso, A. Mascarenhas, S. Froyen, G. S. Horner, K. Bertness, and J. M. Olson, Solid State Commun. **85**, 1021 (1993).

[14] R. G. Alonso, A. Mascarenhas, G. S. Horner, K. A. Bertness, S. R. Kurtz, and J. M. Olson, Phys. Rev. B. **48**, 11 833 (1993).

[15] J. S. Luo, J. M. Olson, S. R. Kurtz, D. J. Arent, K. A. Bertness, M. E. Raikh, and E. V. Tsiper, Phys. Rev. B **51**, 7603 (1995).

[16] J. S. Luo, J. M. Olson, K. A. Bertness, M. E. Raikh, and E. V. Tsiper, J. Vac. Sci. Technol. B **12**, 2552 (1994).

[17] B. A. Philips, I. Kamiya, K. Hingerl, L. T. Florez, D. E. Aspnes, S. Mahajan, and J. P. Harbison, Phys. Rev. Lett. **74**, 3640 (1995).

[18] D. E. Aspnes, J. P. Harbison, A. A. Studna, and L. T. Florez, J. Vac. Sci. Technol. A **6**, 1327 (1988).

[19] K. L. Whittingham, D. T. Emerson, J. R. Shealy, M. Matragrano, and D. G. Ast, Appl. Phys. Lett. **67**, 3741 (1995).

[20] Y. Zhang, P. Ernst, F. A. J. M. Driessen, A. Mascarenhas, C. Geng, F. Scholz, and H. Schweizer, in *Optoelectronic Materials: Ordering, Composition Modulation, and Self-Assembled Structures*, edited by Eric D. Jones, Angelo Mascarenhas, and Pierre Petroff (Materials Research Society, Boston, 1995), p. 61.

[21] V. L. Berkovits, V. A. Kiselev, and V. I. Safarov, Surf. Sci. **211/212**, 489 (1989).

[22] D. J. Friedman, J. G. Zhu, A. E. Kibbler, J. M. Olson, and J. Moreland, Appl. Phys. Lett. **63**, 1774 (1993).

[23] D. J. Friedman, S. R. Kurtz, A. E. Kibbler, K. A. Bertness, C. Kramer, R. Matson, D. L. Arent, and J. M. Olson, in *Evolution of Surface and Thin Film Microstructure*, edited by H. A. Atwatr, E. Chason, M. H. Grabow, and M. G. Lagally (Materials Research Society, Boston, MA, 1993), p. 493.

[24] S. H. Wei and A. Zunger, Phys. Rev. B **51**, 14 110 (1995).

[25] E. P. O'Reilly and A. T. Meney, Phys. Rev. B **51**, 7566 (1995).

[26] Y. Zhang and A. Mascarenhas, Phys. Rev. B **51**, 13 162 (1995).

[27] L. I. Korovin, Fiz. Tverd Tela (Leningrad) **1**, 1311 (1959) [Sov. Phys. Solid State **1**, 1202 (1960)].

[28] J. Callaway, *Quantum Theory of the Solid State* (Academic Press, Boston, 1991).

[29] H. Murata, I. H. Ho, T. C. Hsu, and G. B. Stringfellow, Appl. Phys. Lett. **67**, 3747 (1995).

[30] C. Tanguy, Phys. Rev. Lett. **75**, 4090 (1995).

[31] J. S. Luo, J. M. Olson, and M. C. Wu, J. Vac. Sci. Technol. B **13**, 1755 (1995).

[32] H. Kato, S. Adachi, H. Nakanishi, and K. Ohtsuka, Jpn. J. Appl. Phys. Pt. 1 **33**, 186 (1994).